Tolerance of imperfections in high-energy circular accelerators for polarized protons

S. Y. Lee and E. D. Courant
Accelerator Development Department, Bldg. 1005S, Brookhaven National Laboratory, Associated Universities, Inc., Upton, New York 11973
(Received 20 April 1989)

Realistic calculations show that imperfection-spin-resonance strengths ϵ_{imp} can be corrected to $\epsilon_{imp} < 1$, at 20 TeV, Superconducting Super Collider (SSC) energy. Statistical analysis agrees well with the numerical calculation. The polarized proton must be accelerated through overlapping intrinsic and imperfection resonances. We found a correlation between the tolerable strengths of intrinsic and imperfection resonances ϵ_{int} and ϵ_{imp}, that is, at smaller ϵ_{int}, the tolerable ϵ_{imp} becomes larger, and vice versa. To obtain a larger tolerable ϵ_{imp}, we suggest that the number of snakes should be chosen according to $N_S \geq 5\epsilon_{int}$. When a large number of snakes is used in the accelerator, the tolerable deviation of the spin rotational angle from 180° for each snake becomes more stringent. The error in the spin rotation angle gives rise to (1) an equivalent picket-fence imperfection resonance ϵ_{imp}^{eq} and (2) an energy-dependent spin tune ν_s. Both of these effects may cause depolarization. Further, when the snake axis is not properly arranged, the spin tune deviates from half-integer. In this case, depolarization may arise from the snake resonances. Our analysis indicates that acceleration of polarized protons in the SSC is technically feasible if care is taken in constructing the snakes.

I. INTRODUCTION

Recently, studies were made of the possibilities to obtain polarized proton beams in high-energy accelerators, such as the Relativistic Heavy Ion Collider (RHIC) at Brookhaven National Laboratory (BNL), and the Superconducting Super Collider (SSC).[1] These high-energy accelerators, which include the Tevatron at Fermilab and the SPS at CERN, Geneva, undoubtedly need local spin rotators known as snakes to maintain the beam polarization during acceleration. Analysis of snake configurations, including the allowable tolerance in errors, is important in understanding the mechanism of depolarization during acceleration.

To obtain a polarized beam of protons at high energy, we must first prepare an intense polarized beam and then accelerate it through many depolarizing resonances in a circular accelerator. Depolarization resonances arise either from the vertical betatron motion or from vertical closed-orbit errors. The polarization of the beam is precessed away from its vertical direction by the existing horizontal field of the quadrupoles in the accelerator. Normally, the horizontal fields in the quadrupoles give a small kick to the direction of polarization, unless a resonance condition is encountered. This resonance condition occurs when the spin-precession frequency γG equals the frequency of the depolarization kick, where γ is the Lorentz factor and $G=(g-2)/2$ is the Pauli anomalous magnetic moment. At resonance, the depolarization kicks are coherently in phase each time particles pass through the quadrupole. There are two types of depolarization resonances: (1) intrinsic spin resonances due to the vertical betatron motion, and (2) imperfection spin resonances due to the vertical closed-orbit error. The intrinsic resonances are located[2] at $K=kP\pm\nu_z$, where k is an integer, and P and ν_z are the superperiod and vertical betatron tune of the machine, respectively. The strengths of the important intrinsic resonances increase with energy like $\sqrt{\gamma}\epsilon_N$, where ϵ_N is the vertical normalized emittance ϵ_N, the Courant-Snyder invariant. For SSC, the intrinsic resonance strength is about 5 at 20 TeV and $\epsilon_N = 10\pi$ mm mrad.

Imperfection spin resonances, due to errors in aligning the machine, are located at $K=$integer. The strength of an imperfection spin resonance is, in general, proportional to the closed-orbit error. The relative strength of these resonances depends on the particular distribution of random dipole errors in the machine. However, because of the quasiharmonic betatron motion of particles in the circular accelerator,[3] the closed-orbit distortion is more sensitive to the error harmonic nearest to the vertical betatron tune of the machine. Therefore, the important imperfection spin resonances are located next to the important intrinsic resonances. Fortunately, these imperfection resonances can be controlled by a scheme for proper closed-orbit correction, which is needed for obtaining a proper orbital dynamical aperture, within which particles under the influence of higher multipoles can be confined in the storage mode. The distribution of the imperfection spin resonance will depend on the methods of closed-orbit correction. Nevertheless, the important residual imperfection resonances will still be located next to the important intrinsic resonance (see Sec. II for details).

Since there are both important intrinsic and imperfection spin resonances in a circular accelerator, it is useful to address the question of overlapping resonances.

Recently we made an extensive study of the effects of the snake configurations on the spin resonances.[4] We derived some simple analytic formulas for the strength and location of the dominant spin resonances which depend

on the lattice design of the accelerator, the beam size, and the beam energy. A statistical analysis of the strength of the imperfection spin resonance was made. In this paper we address the question of some basic features of the imperfection resonance after closed-orbit corrections are made.

We also analyzed the snake configuration and the scaling law of the minimum number of snakes versus the spin resonance strength as defined in Ref. 4. For a single intrinsic resonance the maximum strength of spin resonance $\langle \epsilon_c \rangle$ that can be suppressed by a properly chosen snake configuration (away from low-order snake resonances), follows the simple scaling law

$$\langle \epsilon_c \rangle = \frac{\arcsin(|\cos\pi\nu_z|^{1/2})}{\pi} N_S \ , \tag{1}$$

where ν_z and N_S are the vertical betatron tune of the machine and the number of snakes, respectively. The physics of this scaling law is simple: when the spin resonance strength approaches $\langle \epsilon_c \rangle$, the spread of the spin tune overlaps the resonance position. Depolarization occurs because of the multiple crossing of the resonance. Numerical tracking results agree with Eq. (1). For a given accelerator, the resonance strength is known, and one can use Eq. (1) to obtain the minimum number of snakes required. However, in a preliminary study we showed that overlapping intrinsic/imperfection spin resonances would easily cause depolarization at $\epsilon_{\rm int} = \langle \epsilon_c \rangle$, that is, at the critical resonance strength, the polarization will be easily lost if there is an imperfection resonance nearby. Further studies of the overlapping intrinsic and imperfection resonances are needed.

Besides overlapping intrinsic and imperfection resonances, the tolerance of snake imperfections is an important issue. There are two types of snake imperfections: (1) the precession angle is not exactly 180°; and (2) the precession axes of the snake is not in the proper orientation. The first type of imperfection, is equivalent to the imperfection resonance at each integer. We thus expect to obtain similar results as those of the overlapping intrinsic and imperfection resonances. In addition, both types of imperfections give rise to a deviation of spin tune ν_s from the desired $\frac{1}{2}$. Thus, high-order snake resonances may appear.

This paper addresses the tolerance of such imperfections: (1) the imperfection spin resonances, due to error in the particle closed orbit, (2) the error in the spin-rotation angle of each snake, and (3) the error in the spin-rotation axis of each snake. We organize our paper as follows. In Sec. II we evaluate the strength of the imperfection spin resonance before and after the closed-orbit correction. In Sec. III, we study the overlapping intrinsic and imperfection resonances, and discuss the scaling property. In Sec. IV, we explore the tolerance on the snake imperfections. The conclusion is given in Sec. V.

II. THE IMPERFECTION SPIN RESONANCES

Following Eq. (3.1) of Ref. 4 (see also Ref. 2), the spin resonance strength is given by

$$\epsilon_K \simeq \frac{\gamma G}{2\pi} \int_0^{2\pi R} \frac{\partial B_z/\partial x}{B\rho} z e^{iK\vartheta} ds \ , \tag{2}$$

where z is the vertical displacement from the center of a quadrupole and $\partial B_z/\partial x$ is the quadrupole gradient. $B\rho$ is the magnetic rigidity of the particles in the accelerator and γG is the precession frequency of the spin about the vertical axis in one turn around the accelerator in the coordinate system defined in Ref. 4. $2\pi R$ is the circumference of the accelerator. ϵ_K is the resonance strength of the harmonic K, and $\theta \equiv s/\rho$ is the particle's rotational angle around the accelerator.

The vertical displacement z of a particle is composed of two parts:[3] (1) the closed-orbit displacement $z_{\rm CO}$ due to error in dipole field or to misalignment of the quadrupole and (2) the betatron oscillation displacement. The integral due to the betatron displacement gives the strength of the intrinsic spin resonance, located at $K = kP \pm \nu_z$, where P and ν_z are the superperiod and the vertical spin tune of the machine, respectively. The integral due to the closed-orbit displacement gives the strength of the imperfection spin resonance. Because of the betatron motion in the particle accelerator, the closed-orbit distortion $z_{\rm CO}$ is given by

$$z_{\rm CO}(s) = \beta_z^{1/2}(s) \sum_{k=\text{integers}} \frac{\nu_z^2 f_k e^{ik\varphi(s)}}{\nu_z^2 - k^2} \tag{3}$$

with

$$\varphi(s) = \frac{1}{\nu_z} \int \frac{ds}{\beta_z} \ , \tag{4}$$

$$f_k = \frac{1}{2\pi\nu_z} \int_0^{2\pi R} \beta_z^{1/2} \frac{\Delta B}{B\rho} e^{-ik\varphi} ds \ , \tag{5}$$

where $\beta_z(s)$ and $\varphi(s)$ are the vertical betatron amplitude function and the betatron phase. ΔB is the dipole error in the accelerator. The closed orbit $z_{\rm CO}(s)$ in Eq. (3) is more sensitive to the harmonic at $k = \pm[\nu_z]$, the nearest integer to the vertical tune ν_z of the accelerator.

Substituting Eq. (3) into Eq. (2), we obtain[4]

$$\begin{aligned}\epsilon_K = \frac{\gamma G}{2\pi} \sum_{k=\text{integers}} \frac{\nu_z^2 f_k}{\nu_z^2 - k^2} \exp\left[i \frac{P-1}{P} (K+k)\pi \right] \zeta_P \left[\frac{k+K}{P} \right] \\ \times \left\{ \zeta_M \left[\frac{K + k\nu_B/\nu_z}{MP} \right] \{ g_D \beta_z^{1/2}(D) - g_F \beta_z^{1/2}(F) \exp[i(K + k\nu_B/\nu_z)\pi/MP] \} \right. \\ \left. \times \exp\left[i \left[K + k\frac{\nu_B}{\nu_x} \right] \pi/P \right] + X_I \right\} .\end{aligned} \tag{6}$$

Equation (6) is based on the following assumptions. (1) The accelerator is composed of P superperiods, and M FODO cells per superperiod. (2) The dipole magnets are located only in the FODO cell. The vertical betatron phase advance is $2\pi\mu$, and the total betatron tune accumulated through these dipole cells is $\nu_B \equiv MP\mu$. $\beta_z(D)$, $\beta_z(F)$, g_D, and g_F are the vertical betatron amplitude functions, and the corresponding inverse focal length for the defocusing and focusing quadrupole, respectively. (3) The insertion consists of no dipoles. The contribution of the insertion is given by X_I, which depends on the β value at the interaction point and other special properties of the insertions.

The enhancement function $\zeta_N(x)$ describes the coherency of the repeated structure in the circular accelerator: i.e.,

$$\zeta_N(x) \equiv \frac{\sin\pi Nx}{\sin\pi x} \rightarrow N \text{ (at } x = \text{integer)} . \tag{7}$$

Therefore, the resonance strength in Eq. (6) is enhanced P times, due to $\zeta_P[(K+k)/P]$, at

$$K = mP \pm k , \tag{8a}$$

where m is an integer. At the resonance condition of Eq. (8a), each superperiod contributes additively to the total resonance strength. Similarly, the resonance strength is enhanced M times at

$$K = mPM \pm \left[k\frac{\nu_B}{\nu_z} \right], \quad m = \text{integer} , \tag{8b}$$

where each FODO cell accumulates. In a high-energy accelerator, there are many more FODO cells than superperiods, i.e., $M \gg P$. For example, $M \simeq 183$, $P = 2$ in SSC, while in RHIC $M = 24$, $P = 3$. The enhancement due to Eq. (8b) is, therefore, more important than Eq. (8a). When m is an odd integer in Eq. (8b), the effect is even more important, due to the additive kicks of the defocusing and focusing quadrupoles in each FODO cell. When m = even the contributions from the defocusing and focusing quadrupoles in each FODO cells cancel each other out. Thus, there are two distinct enhancement peaks corresponding to m = odd, and two less pronounced peaks for m = even.

Because of the betatron motion, the dominant closed-orbit harmonic k will center around the vertical betatron tune in Eqs. (8). The displacement of the closed orbit due to harmonics k that are far away from the betatron tune shall behave like $1/(k^2 - \nu_z^2)$. The resonance strength, therefore would be smaller. Figure 1 shows the imperfection-resonance strength for SSC before and after the closed-orbit correction by a MICADO correction method.[5] In the lower part of Fig. 1 we show the strength of the intrinsic resonance calculated with a normalized emittance $\epsilon_N = 10\pi$ mm mrad for comparison. Note that the closed-orbit correction can reduce the strength of the imperfection resonance by 2 orders of magnitude, while the displacement of the closed orbit is reduced by 1 order of magnitude. This difference means

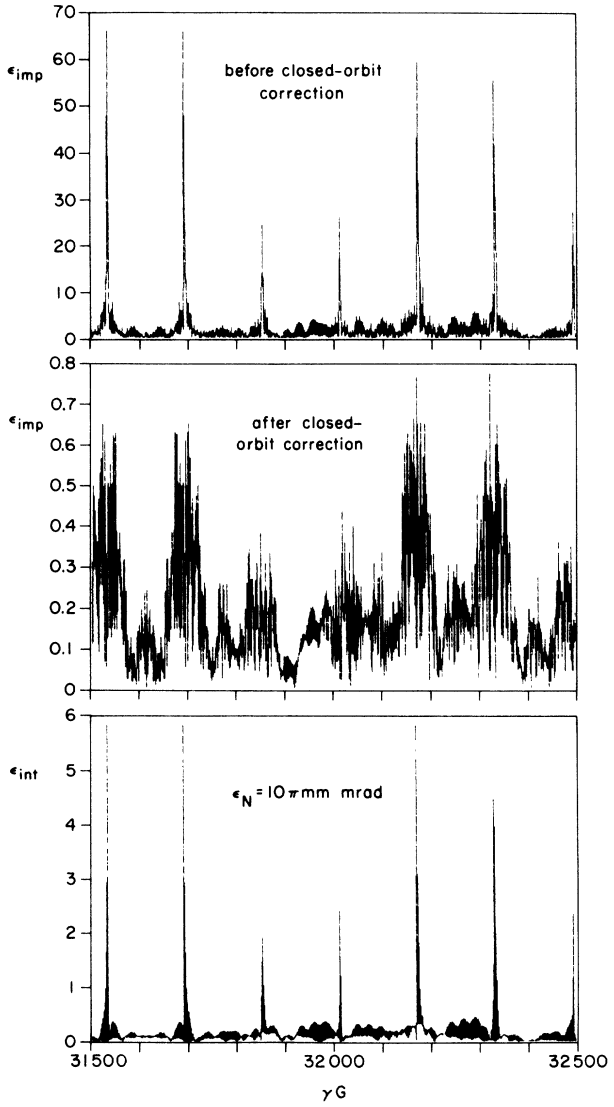

FIG. 1. The imperfection resonance strengths calculated for SSC lattice with quadrupole misalignment rms error of 0.1 mm. The top figure displays the imperfection resonance strength before the closed-orbit correction. The middle figure shows the imperfection resonance strength after the closed-orbit correction to the rms closed-orbit error of 0.3 mm. The important resonance positions are given by Eq. (8b). The corresponding intrinsic resonance for the normalized emittance $\epsilon_n = 10\pi$ mm mrad is shown in the bottom figure for comparisons.

that the closed-orbit correction scheme that was used is more effective for certain harmonics than the others.

We can thus classify the imperfection resonances into two categories: (1) resonance around the betatron tune region and (2) resonances in the background. The dipole error harmonic f_k, near the betatron tune region $k \sim [\nu_z]$ gives a large orbital distortion. Thus, the resonance strength would be very large (see the upper part of Fig. 1). Particles may not be stable in an accelerator with such a large closed-orbit distortion because of the nonlinearity in the magnets. When closed-orbit schemes are

applied, the harmonic around the betatron tune region is minimized, that is, Eq. (3) becomes

$$z_{\rm CO}=\beta_z^{1/2}(s)\sum_{k=\text{integers}} Z_k e^{ik\varphi(s)}\ , \tag{9}$$

where the pole structure of Eq. (3) has disappeared. Statistically, Z_k should be nearly equal around the betatron tune. The harmonic k far away from ν_z, Z_k should still behave like $1/k^2$, because of the quasiharmonic motion of the particle. Thus, after the closed-orbit correction, we would still expect that the harmonics k near to ν_z to have a larger amplitude, Z_k in Eq. (9) than those harmonics far away from ν_z. The closed-orbit correction can decrease markedly the resonance strength at harmonic $k\sim\nu_z$ but cannot change the strength at harmonic k far away from ν_z. Therefore, background resonances will not be affected by the closed-orbit correction. Using a statistical argument, we expect the rms closed-orbit displacement to be given by

$$\langle z_{\rm CO}^2\rangle^{1/2}=\beta_z^{1/2}(s)\sqrt{\nu}\langle Z_k^2\rangle^{1/2}=\frac{1}{\sqrt{2}}\beta_z^{1/2}(s)\sqrt{\nu}\,Z_{k,\max}\ . \tag{10}$$

The resonance strength generated from the closed orbit of Eq. (9) is given by

$$\epsilon_K=\frac{\gamma G}{2\pi}\sum_k Z_k\exp\left[i\pi\frac{P-1}{P}(k+K)\right]\zeta_P\left[\frac{K+k}{P}\right]\times\left[\zeta_M\left[\frac{K+k\nu_B/\nu_z}{MP}\right]\left\{g_D\beta_z^{1/2}(D)-g_F\beta_z^{1/2}(F)\exp\left[i\left[K+k\frac{\nu_B}{\nu_z}\right]\pi/MP\right]\right\}\times\exp\left[i\left[K+k\frac{\nu_B}{\nu_x}\right]\pi/P\right]+X_I\right]\ . \tag{11}$$

Using the estimate of Eq. (10) we obtain

$$\epsilon_{K,\max}\simeq\frac{\gamma G}{2\pi}M\frac{\sqrt{2}\langle Z_{\rm CO}^2\rangle^{1/2}g_D}{\sqrt{\nu}}\left[1+\left[\frac{\beta_z(F)}{\beta_z(D)}\right]^{1/2}\right]\ . \tag{12}$$

For SSC, $\epsilon_{K,\max}\approx 2\times10^3\langle z_{\rm CO}^2\rangle^{1/2}[m]$, when $g_D\approx 0.01\ \text{m}^{-1}$, $M\simeq 183$, $\gamma\simeq 20\,000$, and $\nu\simeq 80$ are used for the estimate. For example, when the closed orbit is corrected to a residual error of $\sigma_{\rm CO}=\langle Z_{\rm Co}^2\rangle^{1/2}\simeq 0.3$ mm, i.e., the maximum closed orbit can be as high as $4\sigma_{\rm CO}\simeq 1.2$ mm, then the maximum strength of the spin resonance is expected to be about $\epsilon_{K,\max}\simeq 0.6$ at 20 TeV.

The above estimate agrees will with the result from a realistic closed-orbit correction shown in Fig. 1. On the other hand, the background contribution should be an order of magnitude smaller, i.e., $\epsilon_K\simeq 0.1$ for K far away from the conditions given in Eq. (8b). The question is the following. What will happen to the polarization when a *bunch* of imperfection resonances of the order of 0.6 are located near to an important intrinsic resonance with strength $\epsilon\simeq 5$ or more? We discuss this question in the next section.

III. OVERLAPPING INTRINSIC AND IMPERFECTION SPIN RESONANCES

Since the important imperfection spin resonance is located near the important intrinsic spin resonance, it is worthwhile to understand the effect of overlapping resonances. Let us review the essential physics on the critical resonance strength $\langle\epsilon_c\rangle$ of Eq. (1).

A. Review on the isolated spin resonance

The spin motion can be solved analytically for a single isolated resonance. Following the notation of Ref. 4, the spin-transfer matrix, defined as the matrix transforming the initial two-component spinor $\psi(\theta_i)$ at orbital angle θ_i to a final spinor $\psi(\theta_f)$ at θ_f as

$$\psi(\theta_f)=t(\theta_f,\theta_i)\psi(\theta_i)\ , \tag{13}$$

where the components of the matrix $t(\theta_f,\theta_i)$ are

$$\begin{aligned} t_{11}(\theta_f,\theta_i)&=ae^{i[c-K(\theta_f-\theta_i)/2]}\ ,\\ t_{12}(\theta_f,\theta_i)&=ibe^{-i[d+K(\theta_f+\theta_i)/2]}\ ,\\ t_{21}(\theta_f,\theta_i)&=-t_{12}^*(\theta_f,\theta_i)\ ,\\ t_{22}(\theta_f,\theta_i)&=t_{11}^*(\theta_f,\theta_i)\ , \end{aligned} \tag{14}$$

with

$$\begin{aligned} b&=\frac{|\epsilon|}{\lambda}\sin\frac{\lambda(\theta_f-\theta_i)}{2}=(1-a^2)^{1/2}\ ,\\ \lambda&=(\delta^2+|\epsilon|^2)^{1/2},\quad \delta=K-\gamma G\ ,\\ c&=\arctan\left[\frac{\delta}{\lambda}\tan\frac{\lambda(\theta_f-\theta_i)}{2}\right],\quad d=\arg\epsilon^*\ . \end{aligned} \tag{15}$$

The polarization of the particle is obtained from the expectation value of the Pauli matrix σ_3 in the spinor wave function, i.e., $\mathbf{S}\equiv\langle\psi|\boldsymbol{\sigma}|\psi\rangle$ and $P=S_3=\langle\psi|\sigma_3|\psi\rangle$. The off-diagional matrix element t_{12} is the depolarization driving term, which is proportional to b. The parameter b oscillates with an amplitude $|\epsilon|/\lambda$. For smaller resonance strength, the perturbing kicks will be correspond-

ingly smaller.

When a snake is introduced in the accelerator, the spinor is transformed locally as

$$\psi(\theta_+)=e^{(i/2)\phi \mathbf{n}_S\cdot\sigma}\psi(\theta_-)\equiv S(\phi_S)\psi(\theta_-)\ , \tag{16}$$

where the snake rotates the spin by an angle ϕ around an axis $\mathbf{n}_S=(\cos\phi_S,\sin\phi_S,0)$ on the horizontal plane. $\sigma=(\sigma_1,\sigma_2,\sigma_3)$ are the Pauli spin matrices. The coordinates for the planar accelerator $\hat{x}$, $\hat{s}$, and $\hat{z}$ are, respectively, the planar outward, the longitudinal axis, and the vertical axis. For a fully excited snake, $\phi=180°$, i.e., the direction of spin is reversed in passing through the snake.

The snakes can be arranged in the accelerator in many different configurations. For an accelerator with N_S snakes, these snakes should be arranged with the conditions

$$\sum_{k=\text{odd}}^{N_S}\theta_{k,k+1}=\sum_{k=\text{even}}^{N_S}\theta_{k,k+1}=\pi\ , \tag{17a}$$

$$\pi\nu_s=\sum_{k=1}^{N_S}(-)^k\varphi_k=(j+\tfrac{1}{2})\pi,\quad j=\text{integer}\ , \tag{17b}$$

where $\theta_{k,k+1}$ is the orbit-bending angle between the kth and $(k+1)$th snakes, and φ_k is the rotational axis of the kth snake. The condition in Eq. (17a) ensures that the spin tune ν_s is independent of the spin-precision frequency γG. The condition in Eq. (17b) is used to define the spin tune ν_s.

For an example with two snakes, their axes should be chosen to be $\varphi_2-\varphi_1=\pi/2$. The one-turn spin transfer matrix $t(\theta_0+2\pi,\theta_0)$ [called one-turn map (OTM)] is given by

$$t_{11}(\theta_0+2\pi,\theta_0)=-e^{i(\varphi_1-\varphi_2)}(1-2b^2e^{i\Phi}\cos\Phi)\ , \tag{18a}$$

$$t_{12}(\theta_0+2\pi,\theta_0)=-2iabe^{-i(c-K\pi+\varphi_2)}\cos\Phi\ , \tag{18b}$$

where $b=(|\epsilon|/\lambda)\sin(\pi\lambda/2)$, $\Phi=K\theta_0+K\pi+d-\varphi_1$, and the quantities c and d are defined in Eq. (15). The spin motion can then be obtained iteratively from the OTM as

$$T(\theta_{n+1})=t(\theta_{n+1},\theta_n)T(\theta_n)\ , \tag{19}$$

where $\theta_{n+1}=\theta_n+4\pi/N_S$. Equation (19) can be solved iteratively in powers of the strength parameter b^2: i.e.,

$$T_{11}=T_{11}^{(0)}+T_{11}^{(1)}+T_{11}^{(2)}+\cdots\ ,$$

$$T_{12}=T_{12}^{(1)}+T_{12}^{(2)}+T_{12}^{(3)}+\cdots\ ,$$

where $T_{11}^{(i)}=O(b^{2i})$ and $T_{12}^{(i)}=O(ab^{2i-1})$. A set of iterative hierarchy equations shown in Ref. 4 can be used to solve Eq. (19) perturbatively. In Appendix A we describe the iterative solution for different configuration of snakes.

Depolarization would occur when the off-diagonal element in the spin transfer matrix $T(\theta_n)$ becomes large after passing through the resonances. There are two leading sources of depolarization: (1) spread on the spin tune and (2) the snake resonances, which are discussed below.

1. *The perturbed spin tune Q_s*

The perturbed spin tune Q_s is given by the trace of the OTM as

$$\cos\pi Q_s=-\cos(\varphi_2-\varphi_1)+2b^2\cos(\Phi+\varphi_1-\varphi_2)\cos\Phi$$
$$=b^2\sin(2\Phi)\ , \tag{20}$$

where $\Phi=K\theta_0+K\pi+d-\varphi_1$ is a characteristic of betatron phase for intrinsic spin resonance with $\varphi_2-\varphi_1=\pi/2$, $K=kP\pm\nu_z$. When $K=$integer, the imperfection resonance, Φ is a constant (modulo 2π). The tune spread becomes

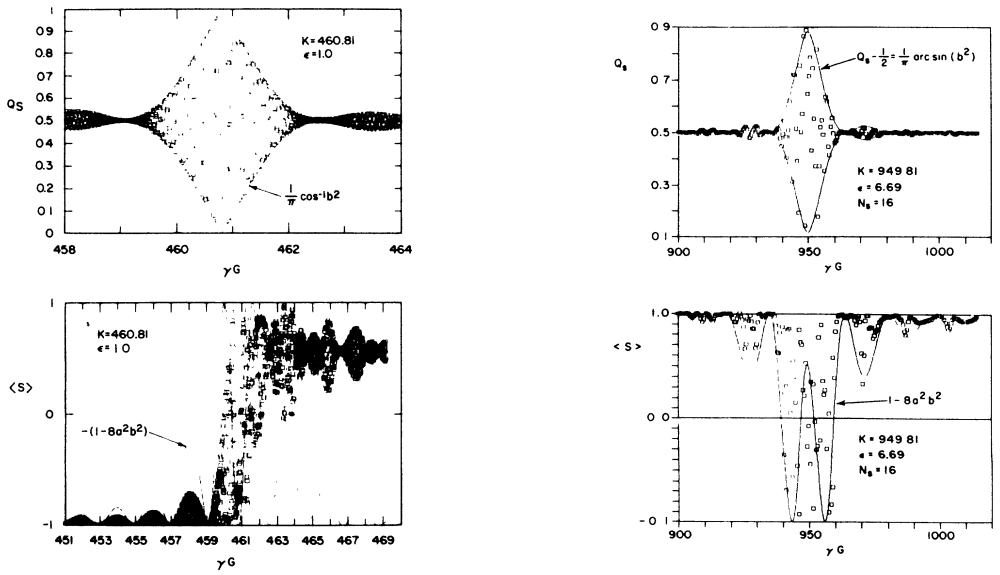

FIG. 2. The spin tracking results for $N_S=2$ and $N_S=16$ are shown, respectively, on the left and right parts of the figure. Appendix A discusses the perturbed spin tune for a large number of snakes. The present example for $N_S=16$ corresponds to $P_S=1$ discussed in Appendix A 2. In the lower part of the figure, the polarization is compared with the envelope function of Eq. (22).

$$Q_s - \tfrac{1}{2} = \frac{1}{\pi}\arcsin b^2 \ . \tag{21}$$

Figure 2 shows the spin-tune spread as the particle being accelerated through the resonance for $N_S=2$ and $N_S=16$. [For $N_S=16$, the parameter b becomes $b=(|\epsilon|/\lambda)\sin(\pi\lambda/N_S)$.] The spin tune oscillates within the envelope of Eq. (21). For $N_S=16$, the $\sin 2\Phi$ in Eq. (20) should be replaced by Eq. (A10) shown in Appendix A. On the other hand, the perturbed spin tune for an imperfection resonance is a smooth function of γG due to $K=$integer and $\sin 2\Phi=$const in the OTM.

We expect that depolarization would occur when the perturbed spin tune overlaps with the resonance frequency at integer $\pm\nu_z$. In such a case, the spin tune may cross the resonance and cause depolarization. Based on the condition of perturbed spin tune, we obtain Eq. (1), which agrees very well with numerical tracking calculations (Fig. 23 of Ref. 4).

2. *The envelope function* $\langle S \rangle$

The polarization is obtained from the expectation value of σ_3 in the spinor wave function, i.e., $S=1-2|T_{12}|^2$. From Eqs. (18) and (19), polarization shall fall within the envelope of

$$\langle S \rangle = 1 - 8a^2b^2 \ . \tag{22}$$

The lower part of Fig. 2 compares the tracking result with the envelope function. The nodal location, where t_{12} of the spin transfer matrix in Eq. (12) becomes zero, corresponds to the spin-matching condition with the snakes.

3. *The snake resonances*

The tolerable resonance is considerably smaller than $\langle \epsilon_c \rangle$ of Eq. (21), when the following conditions of snake resonances are met:[4,6,7]

$$m\nu_s \pm lK = \text{integer}, \quad m,l = \text{odd integers} \ . \tag{23}$$

At the snake-resonance condition, the perturbing kicks to the spin in the spin-tracking equation [Eq. (19)] add up collectively, resulting in depolarization.

We note that the snake-resonance condition Eq. (23) does not include even integer m,l, which is due to cancellation of the linear driving term ($\propto ab$) (Refs. 4, 6, and 7). When $\nu_s \neq \frac{1}{2}$, the cancellation disappears. The even order of Eq. (23), where $m,l=$even integers, appears. These features are discussed in the following sections.

B. Overlapping resonances

We observed that important imperfection resonances are always located near important intrinsic resonances. We studied the overlapping resonance with the following model. For a given isolated intrinsic resonance strength ϵ_{int} the imperfection spin resonances are generated by randomly misaligning the quadrupoles until the spin is depolarized. Figure 3 shows an example of an intrinsic resonance and its nearby imperfection resonances for a random distribution of quadrupole misalignments. The strengths of these imperfection resonances can be adjusted by the amplitude of misalignment.

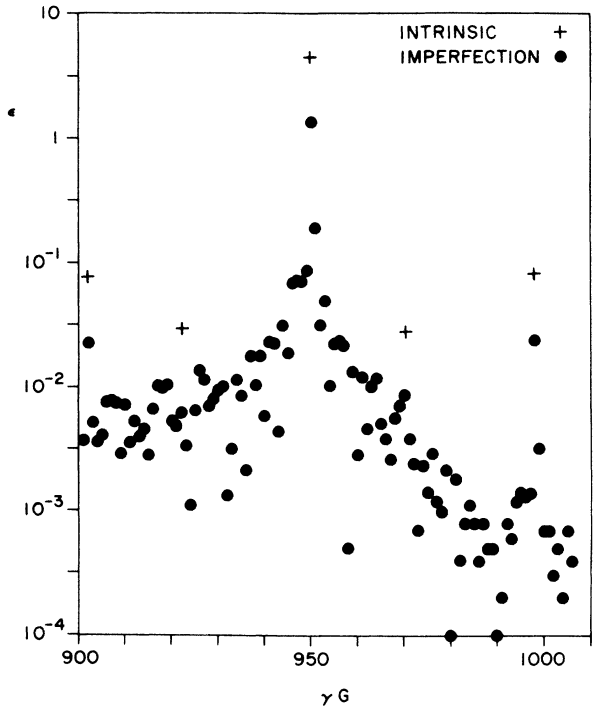

FIG. 3. An example of overlapping intrinsic and imperfection resonances used in the present study.

From the model, a tolerable imperfection resonance strength ϵ_{imp} can be assigned to a given intrinsic resonance strength ϵ_{int}. Figure 4 shows the interrelation between the tolerable imperfection resonance ϵ_{imp} versus the strength of the intrinsic resonance ϵ_{int}. The results show the characteristics of two regions of dominance. When ϵ_{int} [or $\epsilon_{\text{int}}/(N_S/2)$] is near $\langle \epsilon_c \rangle$, the strength of the tolerable imperfection resonance becomes very small, which can be understood through the argument of the perturbed spin tune in Sec. III A 1. When ϵ_{int} is decreased to 0.4, the tolerable imperfection resonance strength ϵ_{imp} becomes larger until $\epsilon_{\text{imp}} \geq 0.3$, where the spin depolarization is dominated by the imperfection spin resonances. A small increase in the imperfection resonance ϵ_{imp} would result in a large reduction in tolerable ϵ_{int}. At $\epsilon_{\text{int}} < 0.025$, where the intrinsic spin resonance can be considered to be insignificant, the strength of the tolerable imperfection resonance is increased suddenly.

In other words, we realized that the linear-order term, proportional to the parameter ab of the spin transfer matrix T in Eq. (19), cancels each other every two turns around the accelerator for $\nu_s=\frac{1}{2}$ and $K=$integer (see Ref. 4 for detail discussion). The tolerable strength of an isolated imperfection spin resonance is, therefore, much larger. When an intrinsic spin resonance is located nearby, the cancellation of the linear order disappeared. A sharp decrease in tolerable ϵ_{imp} is seen in Fig. 4 until $\epsilon_{\text{imp}} \leq 0.3$, when the imperfection spin resonance becomes

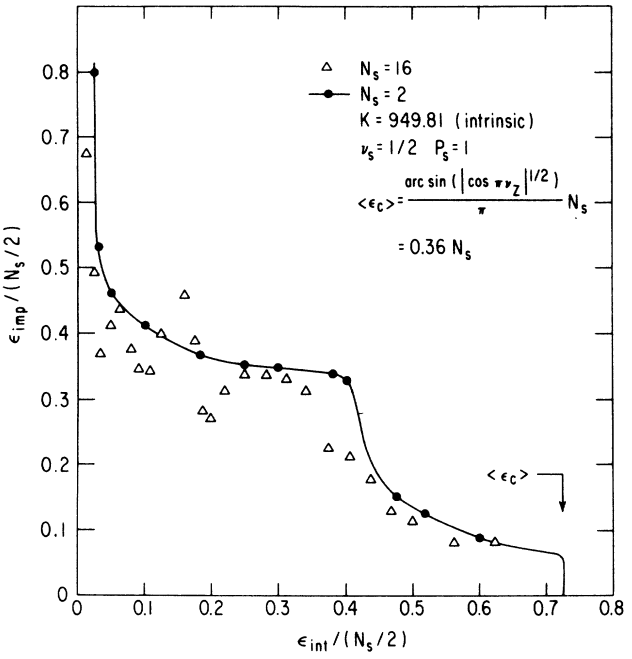

FIG. 4. The correlation between the tolerable intrinsic and imperfection resonance strength. See the text for further discussion.

less important. The tolerable strength of the intrinsic spin resonance can be increased until the perturbed spin tune issue, discussed in Sec. III A 1, dominates the depolarization process shown on Fig. 4.

Figure 4 shows also a similar feature for $N_S=16$. The physics is essentially the same as that of $N_S=2$. Comparing the results of $N_S=2$ and $N_S=16$, we found that the scaling property works well.

The scaling property indicates that the required number of snakes can be estimated from Fig. 4 as

$$\epsilon_{\rm int} \simeq 0.4\frac{N_S}{2} = \tfrac{1}{5}N_S \ . \tag{24}$$

The factor of 0.4 is chosen to increase the tolerable imperfection resonance strength shown in Fig. 4. The spin becomes less susceptible to the imperfection spin resonances. Based on the estimate of Eq. (24), we expect $N_S \geq 5\epsilon_{\rm int} \simeq 26$ for SSC ($\epsilon_{\rm int} \simeq 5$ at 20 TeV and the normalized beam emittance of 10π mm mrad). The tolerable imperfection resonance strength becomes $\epsilon_{\rm imp} \simeq 0.1 N_S = 2.6$. The strength of the imperfection spin resonance strength calculated from an SSC lattice is about 0.6 after a closed-orbit correction to 0.3 mm rms displacement (see Sec. II). The snake configuration can thus restore the polarization after passing through the spin resonance.

IV. THE SNAKE IMPERFECTIONS

Besides the dipole error in the circular accelerator resulting from the depolarizing imperfection spin resonances, the snakes themselves, used for maintaining the polarization, may have imperfections. Because a snake is a superposition of dipole magnets for rotating the spin direction 180° around an axis on the horizontal direction without disturbing the orbital motion outside the snake, there can be two types of imperfections: (1) an error in the spin-rotation angle and (2) an error in the snake's rotation axis.

A. Error in spin-rotation angle in a snake

When the spin-rotation angle ϕ in Eq. (16) is not 180°, the spin transfer matrix of the snake can be expressed as

$$t(\theta_S^+,\theta_S^-) = \exp\left[-i\frac{\Delta\phi}{4}n_S\cdot\sigma\right] \times \exp\left[i\frac{\pi}{2}n_S\cdot\sigma\right]\exp\left[-i\frac{\Delta\phi}{4}n_S\cdot\sigma\right], \tag{25}$$

where $\Delta\phi=\pi-\phi$. Comparing Eq. (14) and Eq. (25) we can derive the equivalent imperfection spin resonance $\epsilon_{\rm imp}^{\rm eq}$ due to the error of spin rotation angle as

$$\epsilon_{\rm imp}^{\rm eq}/(N_S/2) \simeq \frac{\Delta\phi}{\pi} \ . \tag{26}$$

The error in the spin rotation angle is equivalent to the imperfection spin resonance at every integer with equal strength (picket fence).

The error in the spin rotation angle also gives rise to the spin tune oscillation about a half-integer as

$$\cos\pi\nu_s = \cos(\gamma G\pi)\sin^2\frac{\Delta\phi}{2} \tag{27a}$$

for an accelerator with two snakes. The spin closed-orbit vector $\hat{\mathbf{n}}$ would also precess around the vertical axis.

Similarly, for an accelerator with N_S snakes, the spin tune becomes

$$\cos\pi\nu_s \simeq \frac{N_S}{2}\cos(2\gamma G\pi/N_S)\sin^2\frac{\Delta\phi}{2} \ , \tag{27b}$$

to the leading order of $\Delta\phi$. Note that each snake is assumed to contribute coherently to the total spin tune. We expect, therefore, that the spin tune would deviate more from a half-integer in the accelerator with a greater number of snakes. Figure 5 shows the amplitude of the spin tune for $N_S=2$ and 16. In general, the spin rotation angle ϕ may statistically deviate from 180° within certain rms value. We shall expect that the spin tune would be proportional to $\sqrt{N_S}$.

The spin can easily be depolarized by (1) the spin tune, (2) the overlapping between the intrinsic and imperfection resonances, or possibly (3) the snake resonance. Figure 6 shows the result of numerical simulation for a tolerable spin rotation angle ϕ versus the strength of the intrinsic spin resonance. For $N_S=2$, the effect of tune spread due to the error in the snake rotation angle is small. The characteristics of Fig. 6 are similar to those of Fig. 4. The corresponding equivalent imperfection resonance $\epsilon_{\rm imp}^{\rm eq}$ is also similar to that of Fig. 4.

Figure 6 shows also the tolerable error in the spin rotation angle for $N_S=16$. The tolerable error is much small-

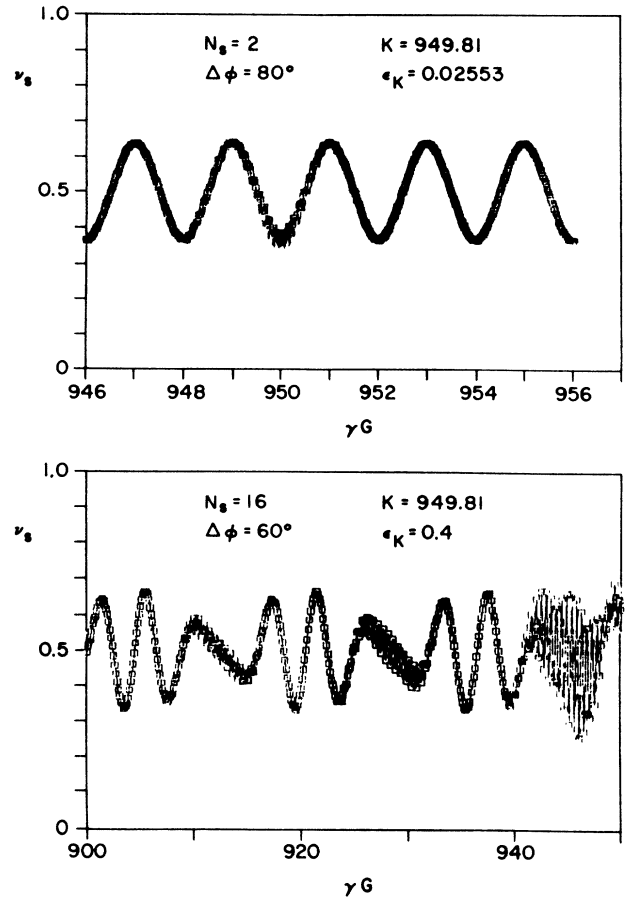

FIG. 5. The spin tune ν_s as a function of γG for the error in spin rotation angle $\Delta\phi$. The spin tune can be obtained perturbatively from Eq. (27b).

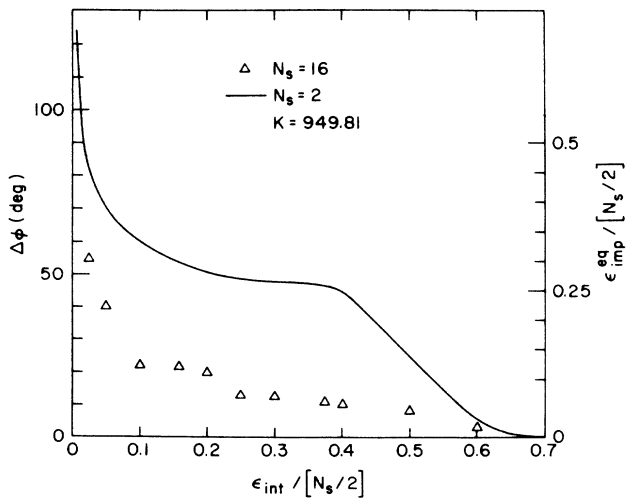

FIG. 6. The tolerable error in the spin-rotation angle $\Delta\phi$ is shown as a function of intrinsic resonance strength. Note that the tolerable error is greatly reduced for a large number of snakes due to spin tune modulation of Eq. (27b).

er, which may be due to the large tune spread for a large number of snakes in Eq. (27b) and Fig. 5.

B. Errors in the snake axis

The axis of spin rotation in each snake in the accelerator should be organized according to Eq. (17b), which gives a half-integer spin tune. However, when the spin rotational axis does not satisfy Eq. (17b), the spin tune would deviate from a half-integer value. By adjusting the relative rotational axis, one can change the spin tune between an integer and half-integer.

Let us consider an example of two snakes, where $\varphi_1 = 0°$ and φ_2 can be adjusted for 0° to 90°; $\pi\nu_s = \varphi_2 - \varphi_1$. The OTM is given by

$$t_{11}(\theta_0 + 2\pi, \theta_0) = -e^{-i\pi\nu_s}(1 - 2b^2 e^{i\Phi}\cos\Phi) , \quad (28a)$$

$$t_{12}(\theta_0 + 2\pi, \theta_0) = -2iabe^{-i(c - K\pi + \varphi_2)}\cos\Phi . \quad (28b)$$

Applying the iterative equation, Eq. (19), we can obtain the nth OTM. Sum up terms which contribute coherently, so that one can obtain again the condition of snake

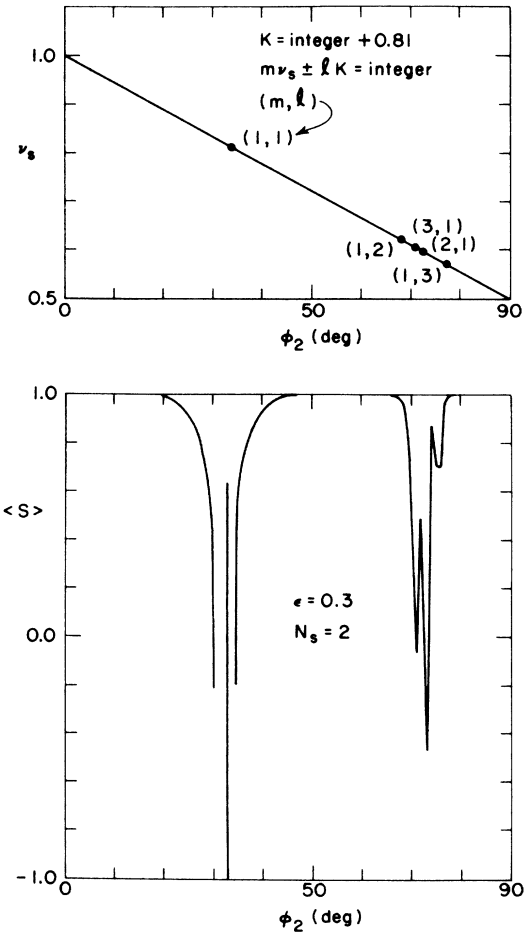

FIG. 7. For accelerators with two snakes, the spin tune is plotted as a function of the spin rotation axis φ_2 with $\varphi_1 = 0$. The position of the snake resonances are also shown. In the lower part of the figure, the polarization after passing through the resonance shows also the effect of the snake resonances.

resonances. Thus, by changing φ_2 relative to φ_1, we observe some snake resonances.[6,7]

Figure 7 shows the final spin $\langle S \rangle$ after passing through a resonance at $K=\text{integer}+0.81$, with $\epsilon=0.3$ as a function of the rotation axis angle ϕ_2 of the second snake (with respect to the radially outward direction). The axis angle for the first snake is chosen to be $\varphi_1=0°$, i.e., radially outward direction. The corresponding spin tune is given by the upper part of Fig. 7, where the snake resonances apparently exist. For a properly chosen vertical betatron tune ν_z, the tolerable imperfection on the snake axis is therefore given by the occurrence of the snake resonance. In the present example with two snakes, we found

$$|\nu_s-\tfrac{1}{2}|\le\tfrac{1}{15}$$

is needed to avoid the low-order snake resonances for $K=\text{integer}+0.81$.

V. CONCLUSION

We have analyzed the tolerance of the imperfection errors in the large hadron accelerator with snakes, and then calculated the imperfection resonance strengths for SSC before and after the closed-orbit correction. Our results agree well with the analytic formula with statistical assumptions. There are two types of imperfection resonance after closed-orbit correction, that is, imperfection resonances near the betatron tune, and background imperfection resonances at harmonics far away from the betatron tune. The strength of the imperfection resonance near the important betatron intrinsic resonance is about 0.6 at 20 TeV after the global closed-orbit correction to a rms closed orbit 0.3 mm. The background imperfection spin resonance is of the order of 0.1, which can be considered to be made up of isolated, small, irrelevant resonances.

We studied also the overlapping intrinsic and imperfection resonances. The tolerable imperfection and intrinsic resonances show the characteristics of two regimes. At $\epsilon_{\text{imp}}/(N_S/2)>0.3$, the tolerable ϵ_{int} is small. Similarly, at $\epsilon_{\text{int}}/(N_S/2)>0.4$, the tolerable ϵ_{imp} is small. Thus, the criteria for the number of snakes should be $N_S\ge 5\epsilon_{\text{int}}$ [Eq. (24)]. The tolerable ϵ_{imp} becomes considerably larger in this region.

We then analyzed the errors on the snakes. The error on the spin rotation angle in the snake can ve viewed as the imperfection resonance. The rotation angle error $\Delta\phi$ can be cast into an equivalent imperfection resonance. The characteristics of Fig. 6 are similar to those of Fig. 4. However, the tolerable error on the spin rotation angle decreases with an increasing number of snakes, possibly due to a large tune spread. Thus, the spin rotation angle is an important consideration in designing the snakes.

Besides the error in the spin rotation angle, the snake axis may not be properly designed. Then, the spin tune would deviate from a half-integer. The limiting feature arises from the snake resonances. Our study shows that the spin tune should not deviate from $\frac{1}{2}$ by more than $\frac{1}{15}$. The corresponding tolerance for the snake axis is about 12°.

Based on our analysis we believe that there is no major difficulty for having a polarized beam in the SSC, where the expected intrinsic resonance strength will be $\epsilon_{\text{int}}\simeq 5$ at $\epsilon_N=10\pi$ mm mrad and $\epsilon_{\text{imp}}\simeq 0.6$ after orbit correction at 20 TeV.

The number of snakes needed is about $N_S\approx 26$. With this number, the effect of the overlapping imperfection resonances should be small (Fig. 4). The spin rotation angle of each snake is important to maintain polarization, and the snake rotation axis should be properly designed to avoid snake resonances.

ACKNOWLEDGMENTS

We thank Dr. A. Woodhead for carefully reading the manuscript. This work was supported under Contract No. DE-AC02-76CH00016 with the United States Department of Energy.

APPENDIX A: SPIN-TUNE SPREAD FOR A LARGE NUMBER OF SNAKES

There are many different snake configurations which satisfy the basic requirement of Eq. (17). The spin motion would depend on the snake configuration. The dependence may render us to a proper choice of the snake configuration. In this appendix we shall study the dependence of the perturbed spin tune in different snake configurations.

The spin transfer matrix at the end of a pair of (φ_2,φ_1) snakes is given by

$$t\left[\theta_0+\frac{4\pi}{N_S},\theta_0\right]=S(\varphi_2)t\left[\theta_0+\frac{4\pi}{N_S},\theta_0+\frac{2\pi}{N_S}\right]\times S(\varphi_1)t\left[\theta_0+\frac{2\pi}{N_S},\theta_0\right], \tag{A1}$$

where $S(\varphi_i)$ is given by Eq. (16) and $t[\theta_0+(n+1)2\pi/N_S,\theta_0+n\cdot 2\pi/N_S]$ is the spin transfer matrix between the nth and the $(n+1)$th snakes given by Eq. (14). The components of Eq. (A1) become

$$t_{11}\left[\theta_0+\frac{4\pi}{N_S},\theta_0\right]=-e^{-i(\varphi_2-\varphi_1)}(1-2b^2e^{i\Phi}\cos\Phi)\ , \tag{A2a}$$

$$t_{12}\left[\theta_0+\frac{4\pi}{N_S},\theta_0\right]=-2iab\exp\left[-i\left[c-\frac{2K\pi}{N_S}+\varphi_2\right]\right]\cos\Phi\ , \tag{A2b}$$

where $\Phi=K\theta_0+2K\pi/N_S+d-\varphi_1$, $b=(|\epsilon|/\lambda)\sin(\pi\lambda/N_S)$, $a=(1-b^2)^{1/2}$, and the quantities c and d are defined in Eq. (15).

The perturbed spin tune Q_s can then be obtained from the trace of the OTM. To obtain the OTM we shall evaluate the spin transfer matrix through the spin tracking equation of Eq. (19). When the number of snakes N_S is large, the OTM becomes rather complicated. We can however solve Eq. (19) perturbatively by using the set of hierarchy equations[4]

$$T_{11}^{(0)}(\vartheta_{n+1})=-e^{i(\phi_1-\phi_2)}T_{11}^{(0)}(\vartheta_n)\ , \tag{A3a}$$

$$T_{12}^{(1)}(\vartheta_{n+1})=-e^{i(\phi_1-\phi_2)}T_{12}^{(1)}(\vartheta_n)-2iabe^{-i\bar{c}}\cos(K\vartheta_n+\bar{d})T_{11}^{(0)*}(\vartheta_n)\ , \tag{A3b}$$

$$T_{11}^{(1)}(\vartheta_{n+1})=-e^{i(\phi_1-\phi_2)}T_{11}^{(1)}(\vartheta_n)+2b^2e^{i(K\vartheta_n+\bar{d}+\varphi_1-\varphi_2)}\cos(K\vartheta_n+\bar{d})T_{11}^{(0)}(\vartheta_n)+2iabe^{-i\bar{c}}\cos(K\vartheta_n+\bar{d})T_{12}^{(1)*}(\vartheta_n)\ , \tag{A3c}$$

$$T_{12}^{(2)}(\vartheta_{n+1})=-e^{i(\phi_1-\phi_2)}T_{12}^{(2)}(\vartheta_n)+2b^2e^{i(K\vartheta_n+\bar{d}+\varphi_1-\varphi_2)}\cos(K\vartheta_n+\bar{d})T_{12}^{(1)}(\vartheta_n)-2iabe^{-i\bar{c}}\cos(K\vartheta_n+\bar{d})T_{11}^{(1)*}(\vartheta_n)\ . \tag{A3d}$$

with $\bar{c}=c-2K\pi/N_S+\varphi_2$ and $\bar{d}=d+2K\pi/N_S-\varphi_1$.

1. Snake configuration with snake superperiod $P_S=N_S/2$

The most simple snake configuration corresponds to $N_S/2$ identical pairs of (φ_2,φ_1) snakes such that

$$\nu_s=N_S(\varphi_2-\varphi_1)/2\pi=j+\tfrac{1}{2}$$

or

$$\varphi_2-\varphi_1=\pi\nu_s/P_S\ .$$

The corresponding snake superperiod is $P_S=N_S/2$. Because of the repeated structure of these pair of snakes we can solve Eq. (19) perturbatively as

$$T_{11}^{(0)}(\theta_n)=(-)^n e^{-in\pi\nu_s/P_S}\ , \tag{A4a}$$

$$T_{12}^{(1)}(\theta_{n+1})=(-)^{n+1}2iab\exp\left[-i\left[c-\frac{k\pi}{P_S}+\varphi_2+n\frac{\pi\nu_s}{P_S}\right]\right]\sum_{m=0}^{n}\exp\left[i\frac{2m\pi\nu_s}{P_S}\right]\cos\left[\Phi+\frac{2m\pi K}{P_S}\right]\ , \tag{A4b}$$

$$\begin{aligned}T_{11}^{(1)}(\theta_{n+1})=&(-)^n2b^2\exp\left[-i\frac{(n+1)\pi\nu_s}{P_S}\right]\sum_{m=0}^{n}\exp\left[i\left[\Phi+\frac{2mK\pi}{P_S}\right]\right]\cos\left[\Phi+\frac{2mK\pi}{P_S}\right]\\&+(-)^n4b^2\exp\left[-i\frac{(n-1)\pi\nu_s}{P_S}\right]\sum_{m=0}^{n-1}\exp\left[i\frac{2\pi m\nu_s}{P_S}\right]\cos\left[\Phi+\frac{2(m+1)K\pi}{P_S}\right]\sum_{l=0}^{m}\cos\left[\Phi+\frac{2lK\pi}{P_S}\right]\\&\times e^{-i2\pi\nu_s l/P_S}\ ,\end{aligned} \tag{A4c}$$

where $\Phi=K\theta_0+2K\pi/N_S+d-\varphi_1$. The first-order term $T_{12}^{(1)}$ in Eq. (A4b) can be summed easily to give

$$\begin{aligned}T_{12}^{(1)}=(-)^{n+1}2iab\exp&\left[-i\left[c-\frac{K\pi}{P_S}+\varphi_2\right]\right]\frac{1}{2}\left\{\exp\left[i\left[\Phi+\frac{n\pi K}{P_S}\right]\right]\zeta_{n+1}\left[\frac{K+\nu_s}{P_S}\right]\right.\\&\left.+\exp\left[-i\left[\Phi+\frac{n\pi K}{P_S}\right]\right]\zeta_{n+1}\left[\frac{K-\nu_s}{P_S}\right]\right\}\ ,\end{aligned} \tag{A5}$$

where the enhancement function $\zeta_n(x)$ is given by Eq. (7). At the conditions $(K\pm\nu_s)/P_S=$integer, which is the first-order snake resonance, the off-diagonal matrix element T_{12} becomes larger. The spacing and the width for the first-order snake resonances increase linearly with P_S. One should choose ν_s and P_S properly to avoid all the important spin resonances, which depends solely on the lattice design of the accelerator.

The perturbed spin tune can be obtained from the trace of $T_{11}(\theta_{P_S})$ of the OTM. From Eq. (A5) with $n+1=P_S$ we obtain then

$$\begin{aligned}\cos\pi Q_s=&\pm b^2\zeta_{P_S}\left[\frac{2K}{P_S}\right]\sin\left[2\Phi+2K\pi-\frac{2K\pi}{P_s}\right]\\&\pm\tfrac{1}{2}b^2\left[\zeta_{P_S-1}\left[\frac{K+\nu_s}{P_S}\right]\left[\frac{\sin[2\Phi+(P_S+1)/\pi\nu_s/P_S+(P_S-1)\pi K/P_S]}{\sin[\pi(K-\nu_s/P_S]}+\frac{\cos[(P_S+1)/\pi(K+\nu_s)P_S]}{\sin[\pi(K+\nu_s/P_S]}\right]\right.\\&+\zeta_{P_S-1}\left[\frac{K-\nu_s}{P_s}\right]\left[\frac{\cos[(P_S+1)/\pi(K-\nu_s)P_S]}{\sin[\pi(K-\nu_s)/P_S]}+\frac{\cos[2\Phi-(\pi\nu_s/P_S)(P_S+1)+(\pi K/P_S)(P_S-1)]}{\cos[\pi(K+\nu_s)/P_S]}\right]\\&-\zeta_{P_S-1}\left[\frac{2K}{P_S}\right]\left[\frac{\cos\{2\Phi+2K\pi-[\pi(K-\nu_s)]/P_S\}}{\sin[\pi(K-\nu_s)/P_S]}+\frac{\cos(2\Phi+3\pi K/P_S-\pi\nu_s/P_S)}{\sin[\pi(K+\nu_s)/P_S]}\right]\\&\left.-(P_S-1)\{\cot[\pi(K-\nu_s)/P_S]+\cot[\pi(K+\nu_s)/P_S]\}\right]\ .\end{aligned} \tag{A6}$$

Thus the perturbed spin tune spread will be large at the conditions $2K/P_S$=integer and $(K\pm\nu_s)/P_S$=integer. The large tune spread in Eq. (A6) may not necessarily give rise to spin depolarization. The spin motion with large tune spread will be more susceptible to the errors discussed in the paper.

When the snake resonance conditions (see Sec. III) are encountered, the $T_{12}^{(1)}$ term in Eq. (A3b) will be large. Therefore the $T_{11}^{(1)}$ term in Eq. (A3c) will also be greatly influenced.

2. Snake configuration with snake superperiod $P_S=1$

The other possible snake configuration has $P_S=1$ by using snakes with different rotation axes φ_n, $n=1,N_S$. Without loss of generality we assume that

$$\varphi_n=(n-1)\frac{2\nu_s\pi}{N_s},\quad n=1,\ldots,N_S\ . \tag{A7}$$

Let $P=N_S/2$. The hierarchy equation (A3) can be solved to obtain the matrix element of the one-turn map as

$$T_{12}^{(1)}(\theta_0+2\pi,\theta_0)=(-)^P 2iab\zeta_P\left[\frac{K-\nu_s}{P}\right]\exp\left[-i\left[c-\frac{K\pi}{P}+\nu_s\pi\right]\right]\cos\left[\Phi_0+\frac{P-1}{P}(K-\nu_s)\pi\right], \tag{A8}$$

$$T_{11}^{(1)}(\theta_0+2\pi,\theta_0)=(-)^{P-1}e^{-i\pi\nu_s}2b^2\left\{\sum_{m=0}^{P-1}\exp\left[i\left[\Phi_0+\frac{2m(K-\nu_s)\pi}{P}\right]\right]\cos\left[\Phi_0+\frac{2m(K-\nu_s)\pi}{P}\right]\right.$$
$$\left.+2\sum_{m=0}^{P-1}\cos\left[\Phi_0+\frac{2m(K-\nu_s)\pi}{P}\right]\sum_{l=0}^{m-1}\cos\left[\Phi_0+\frac{2l(K-\nu_s)\pi}{P}\right]\right\}, \tag{A9}$$

where $\Phi_0=K\theta_0+2K\pi/N_S+d$. The enhancement factor $\zeta_P[(K-\nu_s)/P]$ in the off-diagonal matrix element T_{12} of Eq. (A8) indicates that the depolarization would easily occur at $(K-\nu_s)/P$=integer. Tracking results, shown in Fig. 25 of Ref. 4, display this feature clearly.

From the trace of the diagonal matrix element T_{11} of Eq. (A9) we obtain the perturbed spin tune Q_s as

$$\cos\pi Q_s=\pm b^2\zeta_P\left[\frac{2(K-\nu_s)}{P}\right]\sin\left[2\Phi_0+\frac{2(P-1)}{P}(K-\nu_s)\pi\right]. \tag{A10}$$

One interesting feature of Eq. (A9) is that the second term does not contribute to the perturbed spin tune. The spin tune in the snake superperiod 1 would behave like that of the accelerator with two snakes, provided that the condition $2(K-\nu_s)/P$=integer is avoided.

[1]A. D. Krisch, in *Polarized Beams at SSC*, proceedings of the Workshop, Bodega Bay, California, edited by A. D. Krisch, A. M. T. Lin, and O. Chamberlain (AIP Conf. Proc. No. 145) (AIP, New York, 1985).

[2]E. D. Courant and R. Ruth, BNL Report No. BNL-51270 1980 (unpublished).

[3]E. D. Courant and H. S. Snyder, Ann. Phys. (N.Y.) **3**, 1 (1958).

[4]S. Y. Lee, Report No. BNL-42365 (unpublished).

[5]MICADO, a closed-orbit correction program used in the design of the circular accelerator [B. Antin and Y. Marti, CERN Report No. ISR-MA/73-17 (1973)].

[6]S. Y. Lee and S. Tepikian, Phys. Rev. Lett. **56**, 1635 (1986).

[7]S. Tepikian, Ph.D. thesis, SUNY Stony Brook, 1986.